Supporting Information

Hofmeister Effect-Driven Superlattice Construction *via* Hydrophilic/Hydrophobic Transition of Poly(ethylene glycol) Ligands

Yanqiu Du,[a] Haidong Li,[a] Yang Jiang,[a] Yunchao Xiao,[a] Jipeng Guan,[a] Xuejie Liu,*[a] and Nan Yan*[b]

[a] College of Materials and Textile Engineering, Jiaxing University, Jiaxing 314001, China

[b] Department of Chemistry, Changchun Normal University, Changchun 130032, China

* Corresponding author: E-mail: yannan@ccsfu.edu.cn; 00008109@zjxu.edu.cn

Supplementary Figures

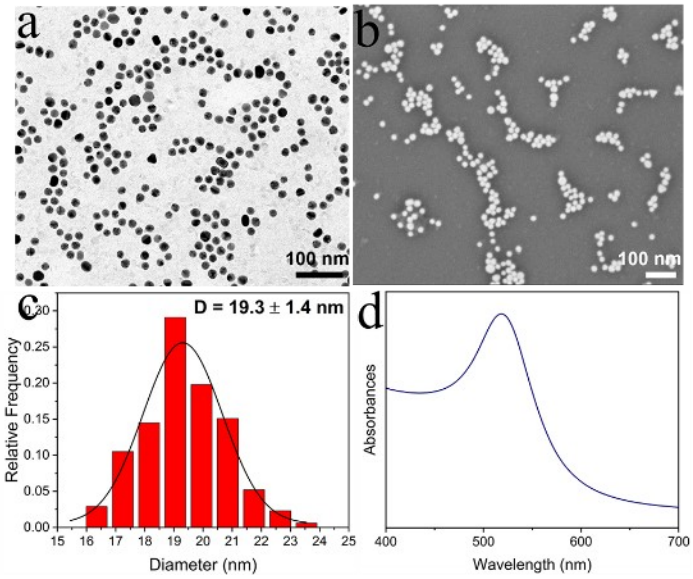

Fig. S1 (a-b) TEM and SEM images of the monodispersed $AuNPs_{19.3}@PEG_{1k}$ building blocks. (c) The size distribution histogram of corresponding $AuNPs_{19.3}@PEG_{1k}$. (d) UV-Vis spectra of the monodispersed $AuNPs_{19.3}@PEG_{1k}$.

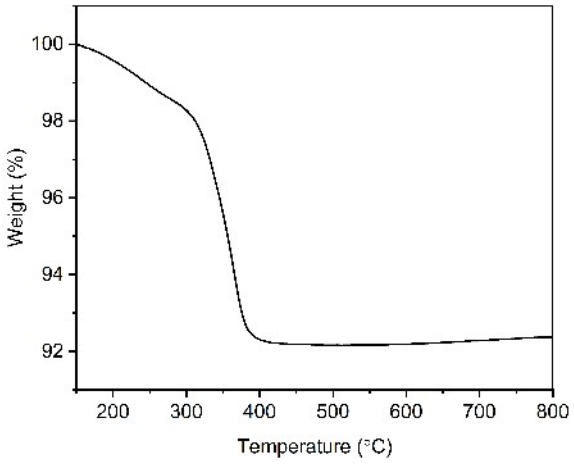

Fig. S2 TGA analysis of the $AuNPs_{19.3}@PEG_{1k}$ nanoparticles.

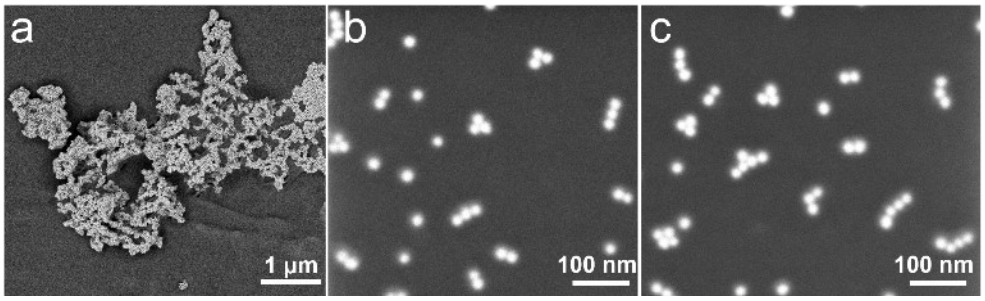

Fig. S3 (a-b) SEM imges of the $AuNPs_{19.3}$ in a 0.60 M K_2CO_3 solution and deionized water, respectively; (c) SEM image of the $AuNPs_{19.3}$@PEG_{1k} in deionized water.

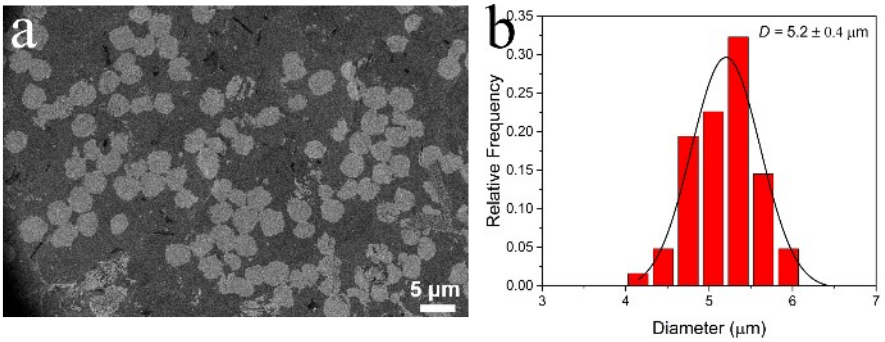

Fig. S4 (a) SEM image of the 2D superlattice sheets at low magnification. (b) The size distribution histogram of corresponding monolayer superlattice sheets.

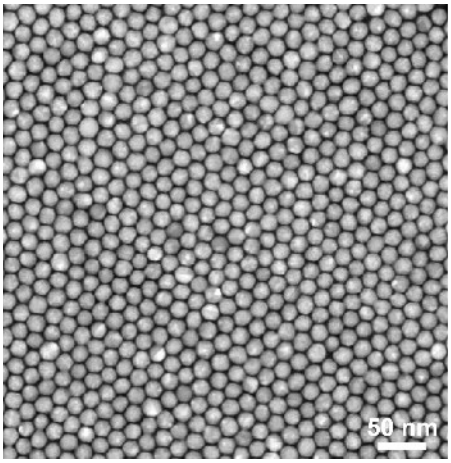

Fig. S5 STEM image of the 2D monolayer superlattice sheets under low magnification.

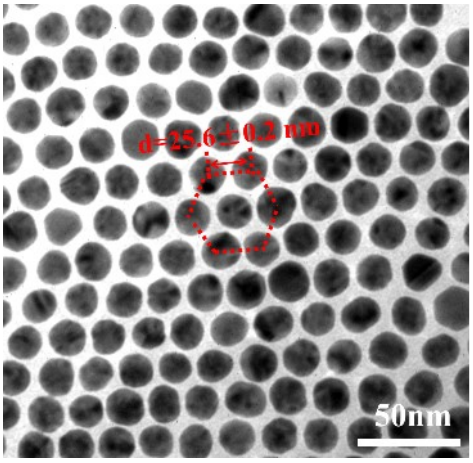

Fig. S6 The interparticle centerpoint-to-centerpoint distances (*d*) in the formed 2D monolayer superlattices are determined by TEM.

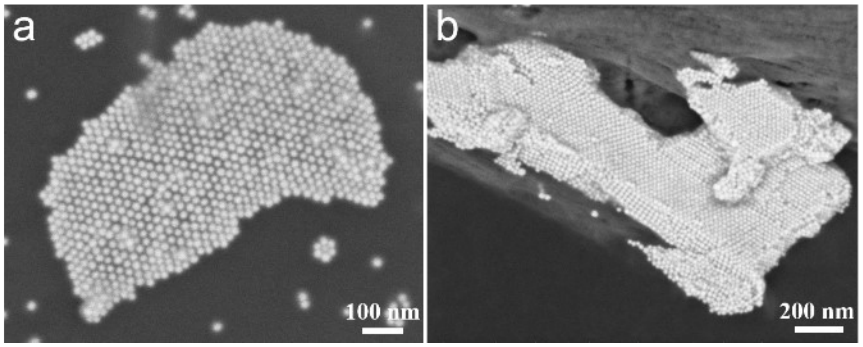

Fig. S7 SEM images of 2D monolayer superlattices (a) and 3D superlattices self-assembled assembled from $AuNPs_{19.3}@PEG_{1k}$ (b) building blocks in a 0.60 M and 0.69 M Na_2CO_3 solution, respectively.

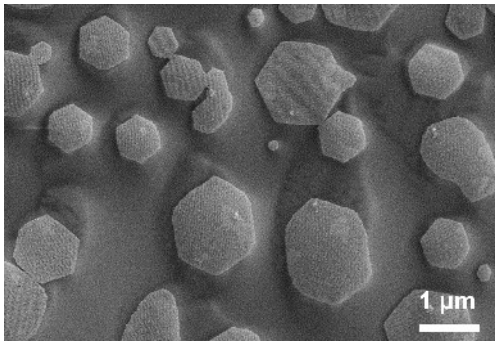

Fig. S8 SEM image of hexagonal monolayer superlattices formed in a 0.69 M K_2CO_3 solution for 12 h.

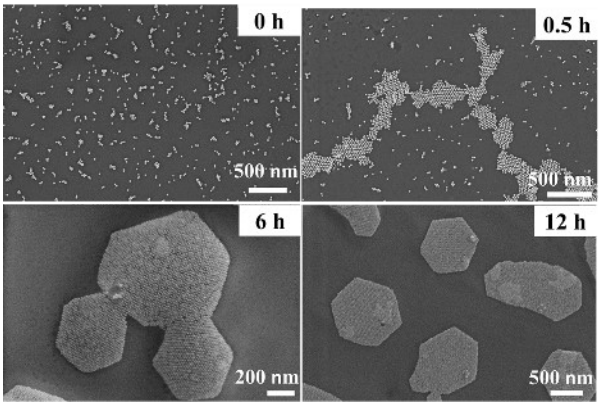

Fig. S9 A sequence of SEM images showing the formation of hexagonal monolayer superlattices formed in a 0.69 M K_2CO_3 solution.

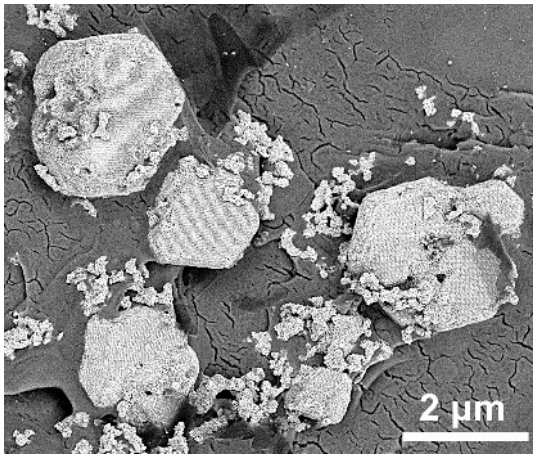

Fig. S10 SEM image of 3D single crystals in a 0.69 M K_2CO_3 solution.

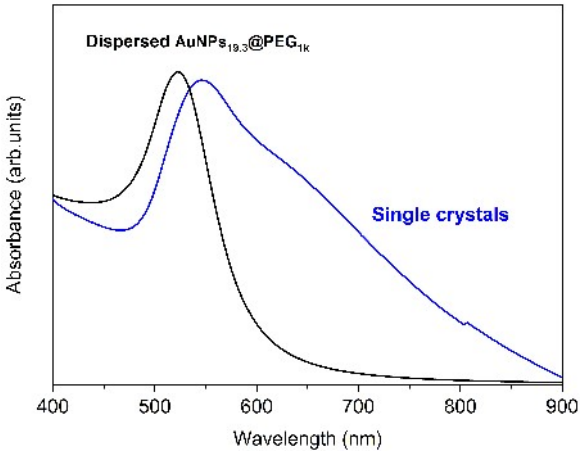

Fig. S11 UV-Vis spectra of dispersed $AuNPs_{19.3}@PEG_{1k}$ (black line) and single crystals self-assembled from $AuNPs_{19.3}@PEG_{1k}$ building blocks (blue line).

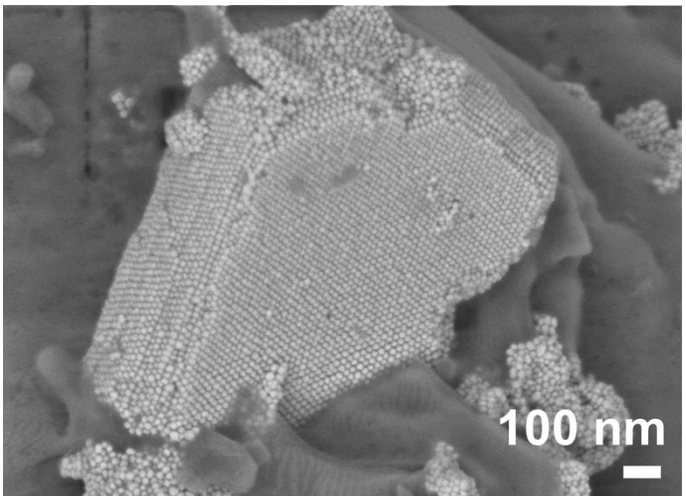

Fig. S12 SEM image of the single crystal obtained in a 0.69 M K_2CO_3 solution when the growth time is 6 h.

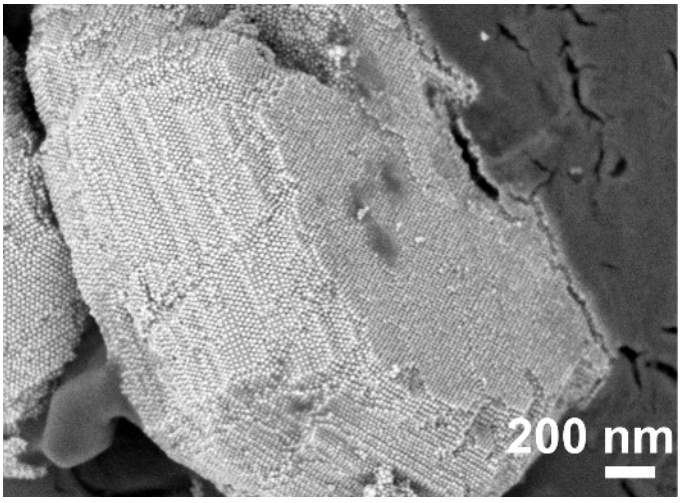

Fig. S13 SEM image of the single crystal obtained in a 0.69 M K_2CO_3 solution when the growth time is 13 h.

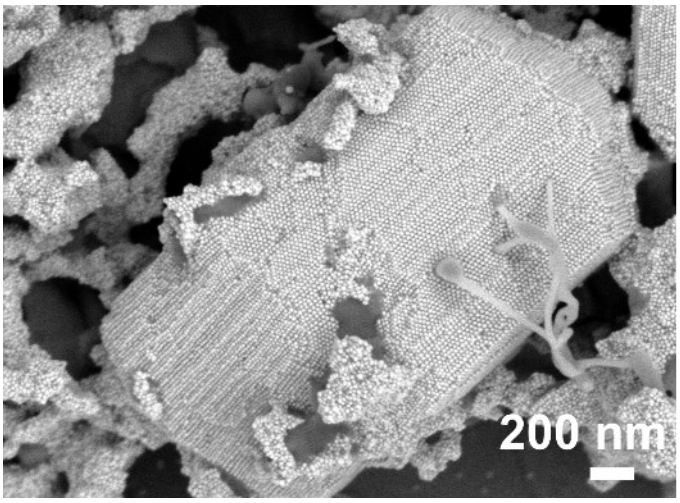

Fig. S14 SEM image of the single crystal obtained in a 0.69 M K_2CO_3 solution when the growth time is 24 h.

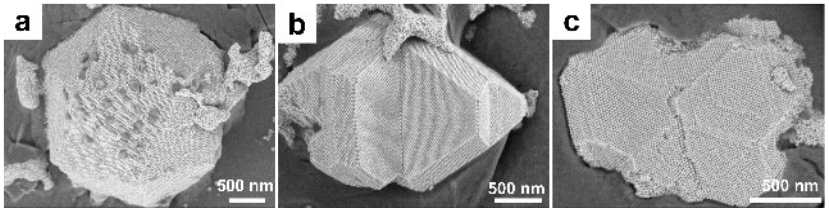

Fig. S15 The formation of multiply twinned superlattices. SEM images of multiply twinned superlattices with quasi-icosahedron (a), a single twin plane (b) and several parallel twin planes (c) that are generated in a 0.85 M K_2CO_3 solution.

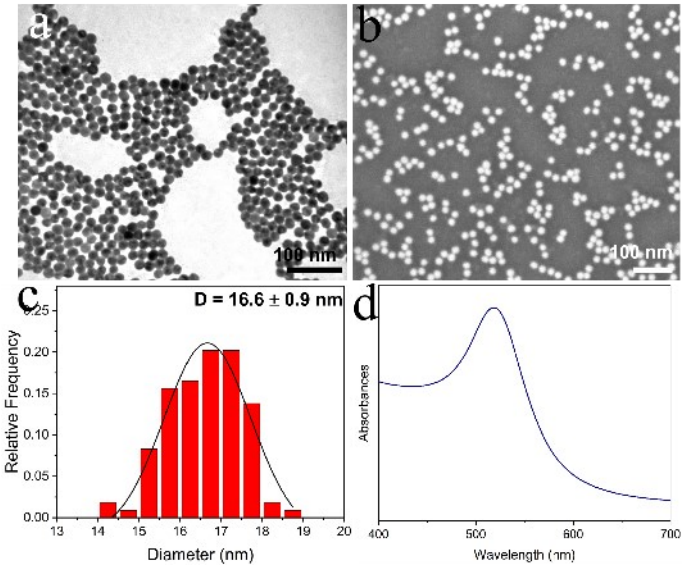

Fig. S16 (a-b) TEM and SEM images of the monodispersed AuNPs with the diameter of 16.6 nm. (c) The size distribution histogram of corresponding $AuNPs_{16.6}$. (d) UV-Vis spectra of the monodispersed $AuNPs_{16.6}$.

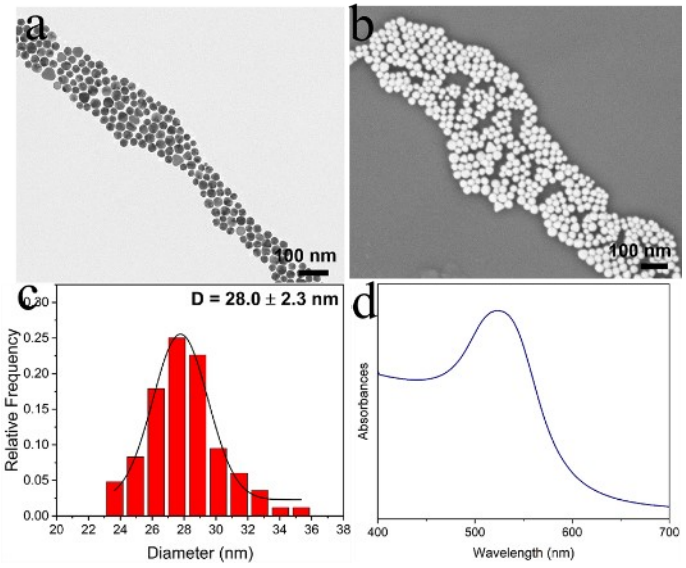

Fig. S17 (a-b) TEM and SEM images of the monodispersed AuNPs with the diameter of 28.0 nm. (c) The size distribution histogram of corresponding $AuNPs_{28.0}$. (d) UV-Vis spectra of the monodispersed $AuNPs_{28.0}$.

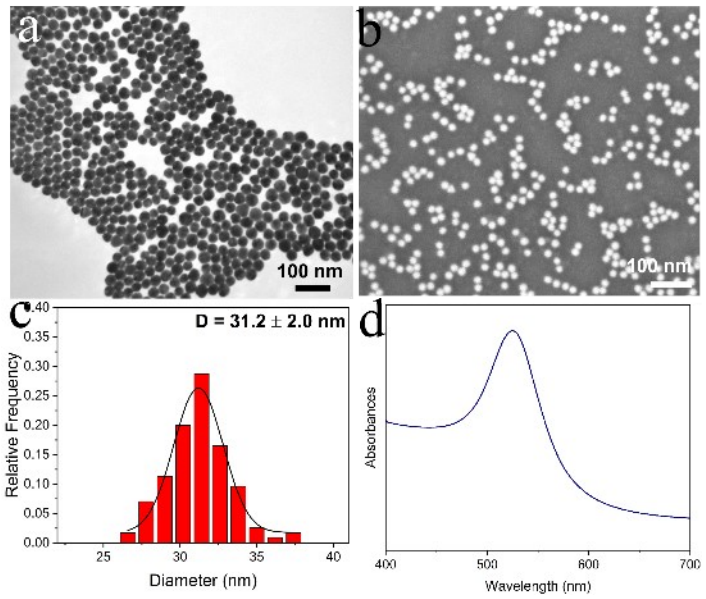

Fig. S18 (a-b) TEM and SEM images of the monodispersed AuNPs with the diameter of 31.2 nm. (c) The size distribution histogram of corresponding $AuNPs_{31.2}$. (d) UV-Vis spectra of the monodispersed $AuNPs_{31.2}$.

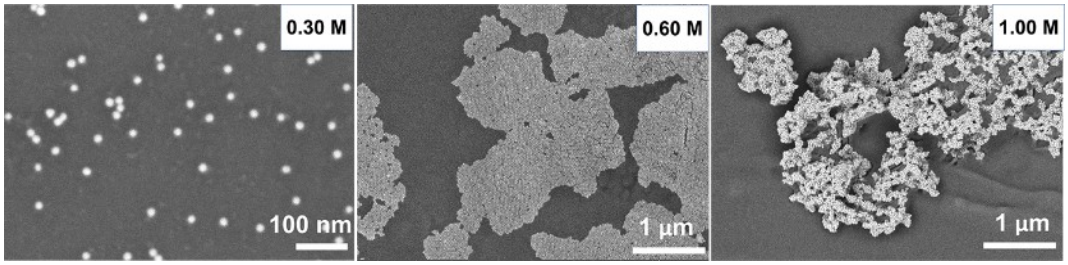

Fig. S19 SEM images of the assembly behavior of $AuNPs_{16.6}$@PEG_{2k} at λ of 0.96 in different K_2CO_3 concentration solution, from left to right are dispersed nanoparticles, monolayer superlattices and disordered aggregates.

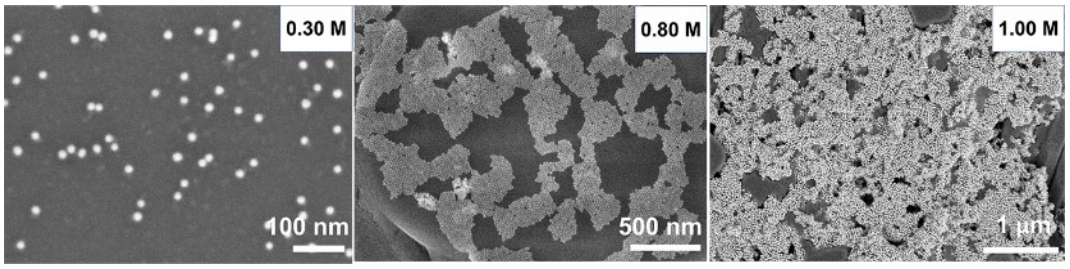

Fig. S20 SEM images of the assembly behavior of $AuNPs_{16.6}@PEG_{5k}$ at λ of 1.55 in different K_2CO_3 concentration solution, from left to right are dispersed nanoparticles, monolayer superlattices and disordered aggregates.

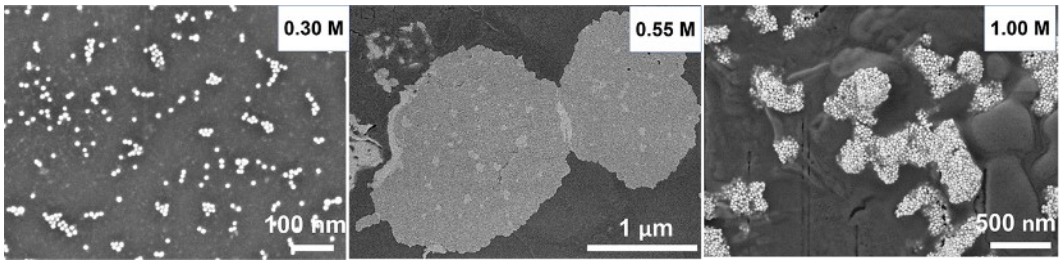

Fig. S21 SEM images of the assembly behavior of $AuNPs_{19.3}@PEG_{2k}$ at λ of 0.83 in different K_2CO_3 concentration solution, from left to right are dispersed nanoparticles, monolayer superlattices and disordered aggregates.

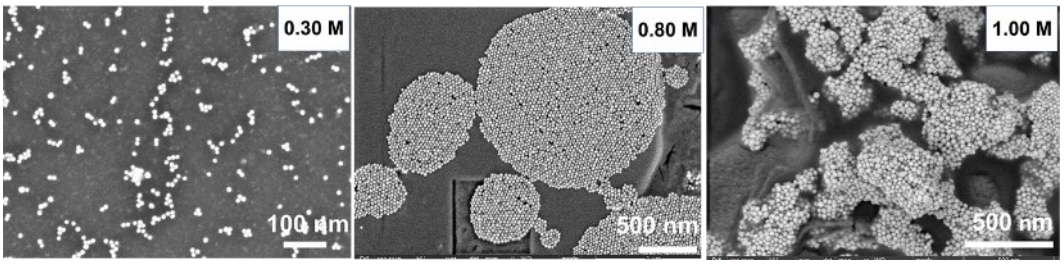

Fig. S22 SEM images of the assembly behavior of $AuNPs_{19.3}@PEG_{5k}$ at λ of 1.35 in different K_2CO_3 concentration solution, from left to right are dispersed nanoparticles, monolayer

superlattices and disordered aggregates.

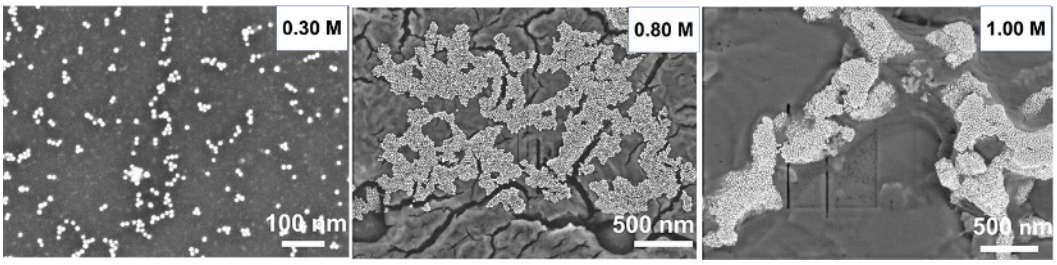

Fig. S23 SEM images of the assembly behavior of $AuNPs_{28.0}@PEG_{5k}$ at λ of 0.93 in different K_2CO_3 concentration solution, from left to right are dispersed nanoparticles, monolayer superlattices and disordered aggregates.

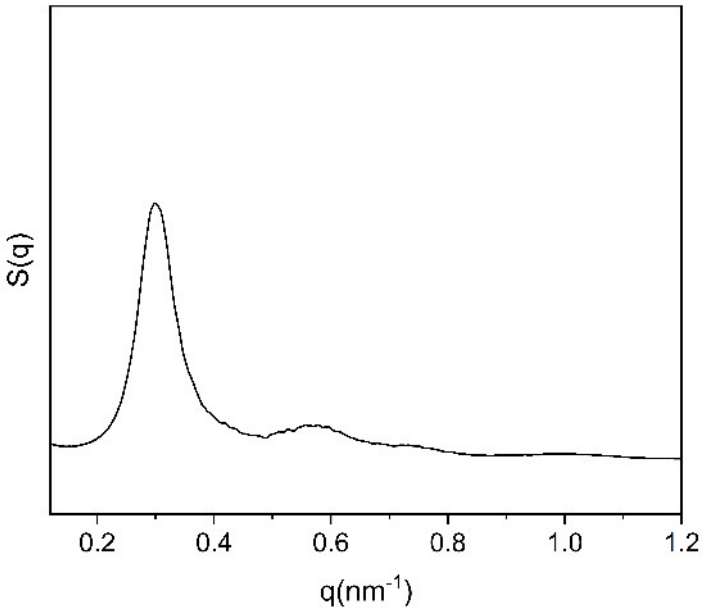

Fig. S24 SAXS pattern of the disordered aggregates assembled from $AuNPs_{16.6}@PEG_{1k}$ building blocks in 1.00 M K_2CO_3 solution.